Current Journal of Applied Science and Technology

40(3): 56-73, 2021; Article no.CJAST.66192
ISSN: 2457-1024
(Past name: British Journal of Applied Science & Technology, Past ISSN: 2231-0843, NLM ID: 101664541)

On the Stability of Collinear Points of the RTBP with Triaxial and Oblate Primaries and Relativistic Effects

S. E. Abd El-Bar[1, 2*]

[1]Mathematics Department, College of Science, Taibah University, Madina, KSA, Saudi Arabia.
[2]Mathematics Department, College of Science, Tanta University, Tanta 31527, Egypt.

Author's contribution

The sole author designed, analyzed, interpreted and prepared the manuscript.

Article Information

DOI: 10.9734/CJAST/2021/v40i331285
Editor(s):
(1) Prof. Qing-Wen Wang, Shanghai University, China.
Reviewers:
(1) Yihu Feng, Shanghai University, China.
(2) Evans Atteh, Wiawso College of Education, Ghana.
Complete Peer review History: http://www.sdiarticle4.com/review-history/66192

Original Research Article

Received 04 January 2021
Accepted 10 March 2021
Published 23 March 2021

ABSTRACT

Under the influence of some different perturbations, we study the stability of collinear equilibrium points of the Restricted Three Body Problem. More precisely, the perturbations due to the triaxiality of the bigger primary and the oblateness of the smaller primary, in addition to the relativistic effects, are considered. Moreover, the total potential and the mean motion of the problem are obtained. The equations of motion are derived and linearized around the collinear points. For studying the stability of these points, the characteristic equation and its partial derivatives are derived. Two real and two imaginary roots of the characteristic equation are deduced from the plotted figures throughout the manuscript. In addition, the instability of the collinear points is stressed. Finally, we compute some selected roots corresponding to the eigenvalues which are based on some selected values of the perturbing parameters in the Tables 1, 2.

Keywords: Collinear points; triaxiality; oblateness; relativistic RTBP; stability.

PACS No: 95.10.Ce

1. INTRODUCTION

The Lagrangian points are very important to the space community as target locations for large space missions, which can be used in many space applications. This needs accurate investigations of the stability of these points. The aim of this paper is to study the linear stability of

**Corresponding author: E-mail: soabdelbar2006@gmail.com;*

the collinear points under effects due to the triaxiality and oblateness of the massive and less massive primaries, respectively. The concerned Restricted Three Body Problem (in brief RTBP) dynamical system is linearized around the equilibrium points. The RTBP studies the motion of a test particle m_3 in the field of two massive bodies m_1 and m_2, which is assumed move in circular orbits about their center of mass, Szebehely [1]. Euler [2] and Lagrange [3] found interesting solutions to the circular RTBP that describe equilibrium positions of the infinitesimal body when all net forces acting on it are zero. Concerning the relativistic effects, the readers can refer to, Brumberg [4,5]. Miandl and Dovrak [6] calculated the advance of perihelion of Mercury's orbit within the framework of the (RTBP), which is the most relevant relativistic effect in the motion of the planets around the Sun. The following researchers Ragos et at. [7] and Douskos and Perdios [8] showed that all collinear points were unstable in agreement with the non-relativistic collinear points. Many authors, such as Ahmed et al., [9], Ishwar and Kushvah [10], Vishnu Namboori et al. [11], Mittal et al. [12], and Kumar and Ishwar [13], Abd El-Salam and Abd El-Bar [14], Abd El-Bar et al, [15], studied the circular RTBP with(out) the relativistic correction, triaxial and oblateness perturbations, and/or radiating. Elshaboury et al, [16], treated RTBP considering the primaries that are triaxial rigid bodies. They concluded that the three collinear equilibrium points are all unstable. Also, they paid special attention to investigate symmetric periodic orbits. Martínez and Simó [17] obtained the totality of relative equilibria as depending on the parameters κ and the mass ratio μ.

The goal of this work is to study the linear stability of collinear equilibrium points with the effects of different combinations of perturbations on stability of collinear points. The rest of this paper is organized as follows: In sec.2, we derived the equations of motion, then we linearized them around the equilibrium points. In sec.3, we discussed the stability of the equilibrium points. While in sec. 4, we outlined the stability of the collinear points. In the subsections 4.1, 4.2, and 4.3 we derived derivatives that are required to study the stability of L_1, L_2 and L_3 respectively. In section 5, we solved the characteristic equation. In sec.6, we gave some stability visualization, and we studied the stability domains in different perturbed cases. Finally, the conclusion was stated in sec.7.

2. RTBP DYNAMICAL EQUATIONS

The motion of an infinitesimal body in the field of our perturbed model of RTBP in dimensionless barycentric-rotating coordinate system are Bhatnagar and Hallan [18].

Where U is the Pseudo-Potential of the problem, m_1, m_2 $(m_1 > m_2)$ and m are the masses of the massive, less massive primaries, and the infinitesimal body, respectively. as shown in the Fig 1.

$$\ddot{\xi} - 2n\dot{\eta} = \frac{\partial U}{\partial \xi} - \frac{d}{dt}\left(\frac{\partial U}{\partial \dot{\xi}}\right), \ddot{\eta} + 2n\dot{\xi} = \frac{\partial U}{\partial \eta} - \frac{d}{dt}\left(\frac{\partial U}{\partial \dot{\eta}}\right) \tag{1}$$

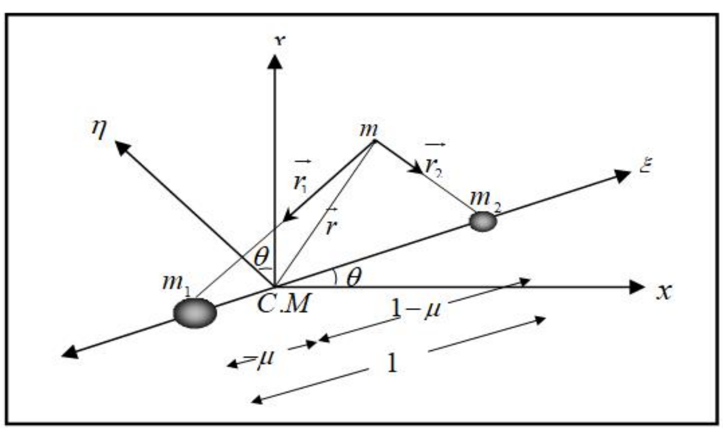

Fig. 1. Geometry for the RTBP

Let $\mu = m_2/m_1 + m_2$ is the small parameter of the problem, $\sigma_i (i = 1,2)$ and $A_2 << 1$ be on respective the numerical values of the coefficients of triaxiality of the massive and oblateness of less massive primaries, c is the speed of light in vacuum.

The Pseudo-Potential function U of the relativistic RTBP is given by

$$\begin{aligned}
U &= \frac{n^2 r^2}{2} + \frac{(1-\mu)}{r_1} + \frac{\mu}{r_2} + \frac{(1-\mu)}{2r_1^3}(2\sigma_1 - \sigma_2) - \frac{3(1-\mu)}{2r_1^5}(\sigma_1 - \sigma_2)\eta^2 - \frac{A_2 \mu}{2r_2^3} \\
&+ \frac{1}{c^2}\left\{ \frac{r^2}{2}(\mu(1-\mu) - 3) + \frac{1}{8}\left[(\dot{\xi} + \eta)^2 + (\dot{\eta} - \xi)^2 \right]^2 \right. \\
&+ \frac{3}{2}\left(\frac{(1-\mu)}{r_1} + \frac{\mu}{r_2} \right)\left[(\dot{\xi} + \eta)^2 + (\dot{\eta} - \xi)^2 \right] - \frac{1}{2}\left(\frac{(1-\mu)}{r_1} + \frac{\mu}{r_2} \right)^2 \\
&\left. - \frac{\mu(1-\mu)}{2}\left[\frac{1}{r_1} + \left(\frac{1}{r_1} - \frac{1}{r_2} \right)(1 - 3\mu - 7\xi - 8\dot{\eta}) + \eta^2 \left(\frac{\mu}{r_1^3} + \frac{(1-\mu)}{r_2^3} \right) \right] \right\}
\end{aligned} \tag{2}$$

where, c is the speed of light, ξ, η are the test particle coordinates in synodic frame of reference. The distance of the test particle from the two massive bodies and from the origin respectively are.

$$r_1 = \sqrt{(\xi + \mu)^2 + \eta^2}, \quad r_2 = \sqrt{(\xi + \mu - 1)^2 + \eta^2}, \quad r = \sqrt{\xi^2 + \eta^2} \tag{3}$$

The perturbed mean motion n is given by

$$n^2 = 1 + \tfrac{3}{2}(2\sigma_1 - \sigma_2) + \tfrac{3}{2}A_2 + \frac{1}{2c^2}(\mu(1-\mu) - 3) \tag{4}$$

The included dynamical variables are made dimensionless according to the following normalization criteria: the sum of masses in the system is normalized as $m_1 + m_2 = 1$, the time is normalized such that unperturbed mean motion $n_0 = 1$. The length is normalized according to considering the distance between the two primaries is unity.

2.1 The Stability of the Collinear Points $L_\alpha, \alpha = 1,2,3$

To study the stability of the orbits near the collinear points, we linearized the equations of motion about the perturbed locations of these points. Let (ξ_o, η_o) be the unperturbed coordinates of $L_\alpha, \alpha = 1,2,3$. They satisfy the equations

$$\ddot{\xi}_0 - 2n\dot{\eta}_0 = \left.\frac{\partial U}{\partial \xi}\right|_{\xi=\xi_o}, \qquad \ddot{\eta}_0 + 2n\dot{\xi}_0 = \left.\frac{\partial U}{\partial \xi}\right|_{\eta=\eta_o} \tag{5}$$

Substituting in equation (1) $\xi = \xi_o + \xi_1$, $|\xi_1| << \xi_0$ and $\eta = \eta_o + \eta_1$, $|\eta_1| << \eta_0$ yields the linearized version of Eq. (1) as

$$\left.\begin{aligned}
\ddot{\xi}_1 - 2n\dot{\eta}_1 &= (U_{\xi\xi})\xi_1 + (U_{\xi\eta})\eta_1 + \ldots \\
\ddot{\eta}_1 + 2n\dot{\xi}_1 &= (U_{\eta\xi})\xi_1 + (U_{\eta\eta})\eta_1 + \ldots
\end{aligned}\right\} \tag{6}$$

where $U_{\xi\xi}=\dfrac{\partial^2 U}{\partial\xi^2}, U_{\xi\eta}=\dfrac{\partial^2 U}{\partial\xi\partial\eta}, U_{\eta\xi}=\dfrac{\partial^2 U}{\partial\eta\partial\xi}$ and $U_{\eta\eta}=\dfrac{\partial^2 U}{\partial\eta^2}$. Retaining 1st order terms in Eq. (6) we obtain linear differential equations with constant. The system (6) has a solution which can be represented as

$$\xi_1 = A e^{\lambda t}, \qquad \eta_1 = B e^{\lambda t} \tag{7}$$

where A and B are constants, and λ are the eigenvalues.

The characteristic equation corresponding to eq. (6) is

$$\lambda^4 - \left(U_{\xi\xi,L_\alpha} + U_{\eta\eta,L_\alpha} - 4\right)\lambda^2 + \left[U_{\xi\xi,L_\alpha} U_{\eta\eta,L_\alpha} - \left(U_{\xi\eta,L_\alpha}\right)^2\right] = 0, \quad \alpha = 1,2,3 \tag{8}$$

where $U_{\xi\xi,L_\alpha}$ and $U_{\eta\eta,L_\alpha}$ are evaluated at the concerned equilibrium point, λ is the roots of the eigenvalue equation (8).

In the collinear points $\eta = 0$, hence $U_{\xi\eta,L_\alpha} = 0$, and the characteristic equation of the system is given by

$$\lambda^4 - \left(U_{\xi\xi,L_\alpha} + U_{\eta\eta,L_\alpha} - 4\right)\lambda^2 + U_{\xi\xi,L_\alpha} U_{\eta\eta,L_\alpha} = 0, \quad \alpha = 1,2,3$$

or

$$\lambda^4 - \mathrm{N}_{L_\alpha} \lambda^2 + \mathrm{M}_{L_\alpha} = 0, \quad \alpha = 1,2,3 \tag{9}$$

where,

$$\mathrm{N}_{L_\alpha} = U_{\xi\xi,L_\alpha} + U_{\eta\eta,L_\alpha} - 4, \qquad \mathrm{M}_{L_\alpha} = U_{\xi\xi,L_\alpha} U_{\eta\eta,L_\alpha} \tag{10}$$

So, the roots of equation (9) are

$$\lambda_{1,2} = \frac{\pm\sqrt{-\mathrm{N}_{L_\alpha} - \sqrt{\left(\mathrm{N}_{L_\alpha}\right)^2 - 4\mathrm{M}_{L_\alpha}}}}{\sqrt{2}}, \qquad \lambda_{3,4} = \frac{\pm\sqrt{-\mathrm{N}_{L_\alpha} + \sqrt{\left(\mathrm{N}_{L_\alpha}\right)^2 - 4\mathrm{M}_{L_\alpha}}}}{\sqrt{2}}, \tag{11}$$

From equation (11) there are three possible solutions for the $\lambda_{1,2}^2$, the first one when $\lambda_{1,2}^2$ is real and negative. In this case two purely imaginary roots $\pm\sqrt{\lambda_{1,2}^2}$ exist, which leads to oscillatory stable solutions, so we will only investigate the case when real $\lambda_{1,2}^2 < 0$. The other two cases when (i) $\lambda_{1,2}^2$ is complex with non-vanishing imaginary part, and (ii) when $\lambda_{1,2}^2$ is real and positive will lead to instability.

These roots can be expressed as $\lambda_{1,2} = \pm\, ib$ and $\lambda_{3,4} = \pm c$ where b and c are real numbers. The product of all root's equals to the constant term in the characteristic equation (i.e., M_{L_α}), this implies that the condition of stability must be

$$\mathrm{M}_{L_\alpha} = U_{\xi\xi,L_\alpha} U_{\eta\eta,L_\alpha} > 0 \tag{12}$$

Substituting $\eta = 0$ into the second order derivatives $U_{\xi\xi,L_\alpha}$ and $U_{\eta\eta,L_\alpha}$ yields,

$$U_{\xi\xi,L_\alpha}=n-\frac{(1-\mu)}{r_1^3}-\frac{\mu}{r_2^3}+3\left[\frac{(1-\mu)(\xi+\mu)^2}{r_1^5}+\frac{\mu(\xi+\mu-1)^2}{r_2^5}\right]-\frac{3A_2\mu}{2r_2^5}$$
$$-\frac{3(1-\mu)(\xi+\mu)(2\sigma_1-\sigma_2)}{2r_1^5}+\frac{15A_2\mu(\xi+\mu-1)^2}{2r_2^7}+\frac{15(1-\mu)(\xi+\mu)^2(2\sigma_1-\sigma_2)}{2r_1^7}$$
$$+\frac{1}{c^2}\left\{(\mu-\mu^2-3)+\frac{3\xi^2}{2}+\left(\frac{(1-\mu)}{r_1}-\frac{\mu}{r_2}\right)\left[\left(\frac{(1-\mu)}{r_1^3}+\frac{\mu}{r_2^3}\right)\right.\right.$$
$$\left.-3\left(\frac{(1-\mu)(\xi+\mu)^2}{r_1^5}+\frac{\mu(\xi+\mu-1)^2}{r_2^5}\right)\right]-\left(\frac{(1-\mu)(\xi+\mu)}{r_1^3}+\frac{\mu(\xi+\mu-1)}{r_2^3}\right)^2$$
$$-6\xi\left(\frac{(1-\mu)(\xi+\mu)}{r_1^3}+\frac{\mu(\xi+\mu-1)}{r_2^3}\right)-\frac{3\xi^2}{2}\left[\left(\frac{(1-\mu)}{r_1^3}+\frac{\mu}{r_2^3}\right)\right.$$
$$\left.-3\left(\frac{(1-\mu)(\xi+\mu)^2}{r_1^5}+\frac{\mu(\xi+\mu-1)^2}{r_2^5}\right)\right]+3\left(\frac{(1-\mu)}{r_1}+\frac{\mu}{r_2}\right)$$
$$-\frac{\mu(1-\mu)}{2}\left[\frac{3(\xi+\mu)^2}{r_1^5}-\frac{1}{r_1^3}+14\left(\frac{(\xi+\mu)}{r_1^3}-\frac{(\xi+\mu-1)}{r_2^3}\right)\right.$$
$$\left.\left.+\left(-1+3\mu+7\xi\right)\left(\frac{3(\xi+\mu)^2}{r_1^5}-\frac{3(\xi+\mu-1)^2}{r_2^5}-\frac{1}{r_1^3}+\frac{1}{r_2^3}\right)\right]\right\} \tag{13}$$

and

$$U_{\eta\eta,L_\alpha}=n-\left(\frac{(1-\mu)}{r_1^3}+\frac{\mu}{r_2^3}\right)-\frac{3A_2\mu}{2r_2^5}-\frac{3(1-\mu)(2\sigma_1-\sigma_2)}{2r_1^5}-\frac{3(1-\mu)(\sigma_1-\sigma_2)}{r_1^5}$$
$$+\frac{1}{c^2}\left\{\left(\frac{(1-\mu)}{r_1}-\frac{\mu}{r_2}\right)\left(\frac{(1-\mu)}{r_1^3}+\frac{\mu}{r_2^3}\right)-(\mu-\mu^2-3)+\frac{\xi^2}{2}\left[1-3\left(\frac{(1-\mu)}{r_1^3}+\frac{\mu}{r_2^3}\right)\right]\right.$$
$$\left.+3\left(\frac{(1-\mu)}{r_1}-\frac{\mu}{r_2}\right)+\frac{\mu(1-\mu)}{2}\left[\frac{1}{r_1^3}-2\left(\frac{(1-\mu)}{r_2^3}+\frac{\mu}{r_1^3}\right)-\left(\frac{1}{r_1^3}-\frac{1}{r_2^3}\right)\left(-1+3\mu+7\xi\right)\right]\right\} \tag{14}$$

2.2 For L_1

Since the considered point is a collinear one, then $\eta=0$. The solution of the classical RTBP satisfies

$$\mathrm{B}_1 r_1+\mathrm{B}_2 r_2=1,\ r_1=\mathrm{B}_1\left(x+\mu\right),\qquad r_2=-\mathrm{B}_2\left(\mu+x-1\right) \tag{15}$$

The L_1 point locates between the two massive primaries and geometry of L_1 can be visualized as given by Fig. 2.

At the point L_1, $\mathrm{B}_1=\mathrm{B}_2=1$ equation (15) becomes

$$r_1+r_2=1,\qquad r_1=\xi+\mu,\qquad r_2=1-\mu-\xi,\qquad \frac{\partial r_1}{\partial\xi}=-\frac{\partial r_2}{\partial\xi}=1 \tag{16}$$

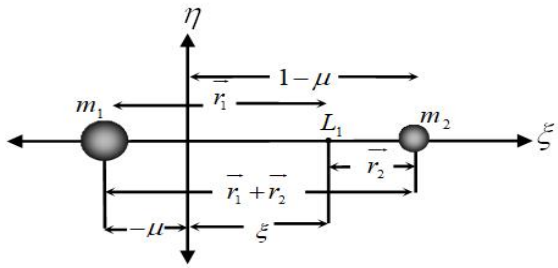

Fig. 2. The location of L_1 and its corresponding parameters

We can assume the position of the L_1 is given by

$$r_1 = a_1 + \delta_{L_1}, \quad r_2 = b_1 - \delta_{L_1}, \quad a_1 + b_1 = 1 \tag{17}$$

From which we have

$$r_1 = (1-b_1)\left(1+\frac{\delta_{L_1}}{1-b_1}\right), \qquad r_2 = b_1\left(1-\frac{\delta_{L_1}}{b_1}\right), \tag{18}$$

where δ_{L_1} is very small a_1 and b_1 are the classical positions of r_1 and r_2, respectively, and b_1 is given by

$$b_1 = \alpha - \frac{1}{3}\alpha^2 - \frac{1}{9}\alpha^3 - \frac{23}{81}\alpha^4 + O\left(\alpha^5\right), \qquad \alpha = \left(\frac{\mu}{3(1-\mu)}\right)^{1/3}. \tag{19}$$

After some lengthy algebraic manipulation, the location of L_1 is

$$\begin{aligned}\xi_{o,L_1} = \sum_{k=-3}^{9} \mathrm{F}_{-k}^{(1)} - \frac{1}{c^2}\Bigg\{ & -\frac{1}{3}(\frac{\mu}{3})^{\frac{1}{3}} + \frac{5}{9}(\frac{\mu}{3})^{\frac{2}{3}} - \frac{4}{3}(\frac{\mu}{3}) + \frac{2425}{486}(\frac{\mu}{3})^{\frac{4}{3}} - \frac{1729}{486}(\frac{\mu}{3})^{\frac{5}{3}} \\ & - \frac{6395}{2187}(\frac{\mu}{3})^2 + \frac{398335}{336366}(\frac{\mu}{3})^{\frac{7}{3}} + \frac{422957}{59049}(\frac{\mu}{3})^{\frac{8}{3}} - \frac{8374501}{354294}(\frac{\mu}{3})^3 + \ldots \Bigg\}\end{aligned} \tag{20}$$

where non-vanishing coefficients $\mathrm{F}_{-k}^{(1)}$ are given Appendix A

Substituting from equations (18) into equations (13) and (14), yields

$$\begin{aligned} U_{\xi\xi,L_1} &= n + 2\left[(1-\mu)(1-3D_1\delta_{L_1})T_1 + S_1\mu(1+3E_1\delta_{L_1})\right] \\ &+ 6\left[\mu G_1 A_2(1+5E_1\delta_{L_1}) + (1-\mu)(2\sigma_1-\sigma_2)(1-5D_1\delta_{L_1})Q_1\right] + \frac{1}{c^2}\Bigg\{\frac{3(1-b_1-\mu)^2}{2} \\ &\times\left[1+2\left(T_1(1-\mu)+S_1\mu\right)\right] + (\mu-\mu^2-3) + 6(1-b_1-\mu)\left[F_1\mu - H_1(1-\mu)\right] + 3\left[E_1\mu + D_1(1-\mu)\right] \\ &- \left[J_1\mu^2 - 2\mu H_1 + F_1(1-\mu) + W_1(1-\mu)^2\right] - 2\left[S_1\mu - T_1(1-\mu)\right]\left[E_1\mu + D_1(1-\mu)\right] \\ &- \frac{\mu(1-\mu)}{2}\left[2T_1 + 2(-6+4\mu+7b_1)(S_1-T_1) + 14(F_1+H_1)\right]\Bigg\} \end{aligned} \tag{21}$$

and

$$\begin{aligned}U_{\eta\eta,L_1} &= n-\left[(1-\mu)(1-3D_{L_1}\delta_{L_1})T_1+S_1\mu(1+3E_1\delta_{L_1})\right]\\&-\frac{3}{2}\left[\mu G_1A_2(1+5E_1\delta_{L_1})+(1-\mu)(2\sigma_1-\sigma_2)(1-5D_1\delta_{L_1})Q_1\right]-3(1-\mu)(\sigma_1-\sigma_2)(1-5D_1\delta_{L_1})Q_1\\&+\frac{1}{c^2}\left\{\frac{(1-b_1-\mu)^2}{2}\left[1-3\left(T_1(1-\mu)+S_1\mu\right)\right]+(\mu-\mu^2-3)\right.\\&+3\left[E_1\mu-D_1(1-\mu)\right]+\left[S_1\mu-T_1(1-\mu)\right]\left[E_1\mu+D_1(1-\mu)\right]\\&\left.-\frac{\mu(1-\mu)}{2}\left[-T_1+(-6+4\mu+7b_1)(S_1-T_1)+2\left(S_1(1-\mu)+T_1\mu\right)\right]\right\}\end{aligned} \tag{22}$$

Where $D_1, E_1, F_1, G_1, H_1, J_1, Q_1, S_1, T_1$ and W_1 are all functions of μ

2.3 For L_2

The L_2 point lie on x-axis on far side of each primary with respect to the barycenter. The geometry of L_2 can be visualized as given by Fig. 3.

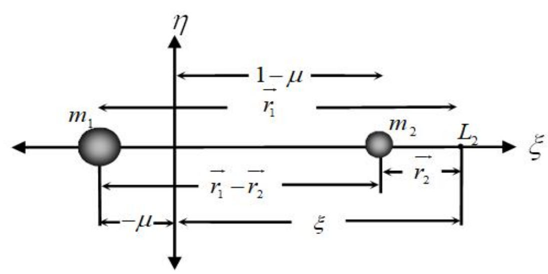

Fig. 3. The location of L_2 and its corresponding parameters

Follow the same procedure as done in L_1, with the corresponding values of $B_1 = 1,\ B_2 = -1$ into (15) we get

$$r_1 - r_2 = 1, \qquad r_1 = \xi + \mu, \qquad r_2 = \xi + \mu - 1, \qquad \frac{\partial r_1}{\partial \xi} = \frac{\partial r_2}{\partial \xi} = 1 \tag{23}$$

The perturbed position of L_2 could be written as a little deviation δ_{L_2} from the classical position as

$$r_1 = a_2 + \delta_{L_2},\ \ r_2 = b_2 - \delta_{L_2},\ \ a_2 + b_2 = 1 \tag{24}$$

From which we have

$$r_1 = (1+b_2)\left(1+\frac{\delta_{L_2}}{1+b_2}\right), \qquad r_2 = b_2\left(1+\frac{\delta_{L_2}}{b_2}\right), \tag{25}$$

where a_2 and b_2 are unperturbed positions of r_1 and r_2, respectively, and b_2 is given by

$$b_2 = \alpha + \frac{1}{3}\alpha^2 - \frac{1}{9}\alpha^3 - \frac{31}{81}\alpha^4 + O\left(\alpha^5\right), \qquad \alpha = \left(\frac{\mu}{3(1-\mu)}\right)^{1/3}. \tag{26}$$

After some lengthy algebraic manipulation, the location of L_2 is

$$\xi_{o,L_2} = \sum_{k=-3}^{9} \mathrm{G}_{-k}^{(2)} + \frac{1}{c^2}\left\{ -\frac{1}{3}(\frac{\mu}{3})^{\frac{1}{3}} - \frac{5}{9}(\frac{\mu}{3})^{\frac{2}{3}} - \frac{4}{3}(\frac{\mu}{3}) + \frac{1084}{486}(\frac{\mu}{3})^{\frac{4}{3}} + \frac{886}{243}(\frac{\mu}{3})^{\frac{5}{3}} \right.$$
$$\left. - \frac{8843}{2178}(\frac{\mu}{3})^2 - \frac{12796}{19683}(\frac{\mu}{3})^{\frac{7}{3}} + \frac{2872}{59049}(\frac{\mu}{3})^{\frac{8}{3}} - \frac{1915435}{354294}(\frac{\mu}{3})^3 + \ldots \right\}$$
(27)

Where non-vanishing coefficients $\mathrm{G}_{-k}^{(2)}$ are given appendix B

Substituting eq. (25) into eq. (13) and (14), yields

$$U_{\xi\xi,L_2} = n + 2\left[(1-\mu)(1-3D_2\delta_{L_2})T_2 + S_1\mu(1-3E_2\delta_{L_2})\right]$$
$$+6\left[\mu G_2 A_2(1-5E_2\delta_{L_2}) + (1-\mu)(2\sigma_1-\sigma_2)(1-5D_2\delta_{L_2})Q_2\right]$$
$$+\frac{1}{c^2}\left\{\frac{3(1-b_2-\mu)^2}{2}\left[1+2\left(T_2(1-\mu)+S_2\mu\right)\right] + (\mu-\mu^2-3)\right.$$
$$-6(1-b_2-\mu)\left[F_2\mu - H_2(1-\mu)\right] + 3\left[E_2\mu + D_2(1-\mu)\right]$$
$$-\left[J_2\mu^2 + 2\mu H_2 + F_2(1-\mu) + W_2(1-\mu)^2\right] - 2\left[S_2\mu + T_2(1-\mu)\right]\left[E_2\mu + D_2(1-\mu)\right]$$
$$\left. -\frac{\mu(1-\mu)}{2}\left[2T_2 + 2(-6+4\mu+7b_2)(S_2-T_2) + 14(F_2+H_2)\right]\right\}$$
(28)

and

$$U_{\eta\eta,L_2} = n - \left[(1-\mu)(1-3D_{L_2}\delta_{L_2})T_2 + S_2\mu(1-3E_2\delta_{L_2})\right]$$
$$-\frac{3}{2}\left[\mu G_2 A_2(1-5E_2\delta_{L_2}) - (1-\mu)(2\sigma_1-\sigma_2)(1-5D_2\delta_{L_2})Q_2\right]$$
$$+3(1-\mu)(\sigma_1-\sigma_2)(1-5D_2\delta_{L_2})Q_2$$
$$+\frac{1}{c^2}\left\{\frac{(1-b_2-\mu)^2}{2}\left[1-3\left(T_2(1-\mu)+S_2\mu\right)\right] - (\mu-\mu^2-3)\right.$$
$$+3\left[E_2\mu + D_2(1-\mu)\right] + \left[S_2\mu + T_2(1-\mu)\right]\left[E_2\mu + D_2(1-\mu)\right]$$
$$\left. +\frac{\mu(1-\mu)}{2}\left[T_2 + (6-4\mu+7b_2)(S_2-T_2) - 2\left(S_2(1-\mu)+T_2\mu\right)\right]\right\} \tag{29}$$

where $D_2, E_2, F_2, G_2, H_2, J_2, Q_2, S_2, T_2$ and W_2 are all functions of μ .

2.4 For L_3

The L_3 point lie on the negative $x-$axis, the geometry of L_3 can be visualized as given by Fig. 4.

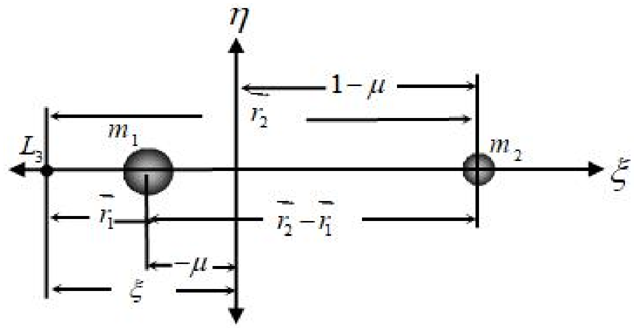

Fig. 4. The location of L_3 and its corresponding parameters

Follow the same procedure as done in L_1, with the corresponding values of $B_1 = -1,\ B_2 = 1$ into (15) we get

$$r_2 - r_1 = 1, \qquad r_1 = -\xi - \mu, \qquad r_2 = 1 - \mu - \xi, \qquad \frac{\partial r_1}{\partial \xi} = \frac{\partial r_2}{\partial \xi} = -1 \tag{30}$$

Proceeding similarly as before following the same steps

$$r_1 = a_3 + \delta_{L_3},\ \ r_2 = b_3 - \delta_{L_3},\ \ a_3 + b_3 = 1 \tag{31}$$

From which we have

$$r_3 = -(1-b_3)\left(1 - \frac{\delta_{L_3}}{1-b_3}\right), \qquad r_2 = b_3\left(1 + \frac{\delta_{L_3}}{b_3}\right), \tag{32}$$

where a_3 and b_3 are unperturbed positions of r_1 and r_2 respectively, and b_3 is given by

$$b_3 = 2 - \frac{7}{12}\mu\left(1 + \frac{23}{144}\mu + \frac{25921}{2985984}\mu^4\right) \tag{33}$$

After some lengthy algebraic manipulation, the location of L_3 is

$$\xi_{o,L_3} = \sum_{k=-3}^{9} \mathrm{J}_{-k}^{(3)} - \frac{1}{c^2}\left\{-\frac{3}{4}\mu + \frac{7}{16}\mu^2 + \frac{3227}{41472}\mu^3 + \frac{51037}{497664}\mu^5 + \dots\right\} \tag{34}$$

Where non-vanishing coefficients $\mathrm{J}_{-k}^{(3)}$ are given appendix C

Substituting eq. (32) into eq. (13) and (14), yield

$$U_{\xi\xi,L_3} = n + 2\left[(1-\mu)(1-3D_3\delta_{L_3})T_3 + S_3\mu(1-3E_3\delta_{L_3})\right]$$
$$+6\left[\mu G_3 A_2(1-5E_3\delta_{L_3}) + (1-\mu)(2\sigma_1-\sigma_2)(1-5D_3\delta_{L_3})Q_3\right]$$
$$+\frac{1}{c^2}\left\{\frac{3(1-b_3-\mu)^2}{2}\left[1+2\left(T_3(1-\mu)+S_3\mu\right)\right] + (\mu-\mu^2-3)\right.$$
$$+6(1-b_3-\mu)\left[F_3\mu + H_3(1-\mu)\right] + 3\left[E_3\mu + D_3(1-\mu)\right]$$
$$-\left[J_3\mu^2 + 2\mu H_3 + F_3(1-\mu) + W_3(1-\mu)^2\right] - 2\left[S_3\mu + T_3(1-\mu)\right]\left[E_3\mu + D_3(1-\mu)\right]$$
$$\left.-\frac{\mu(1-\mu)}{2}\left[2T_3 + 2(-6+4\mu+7b_1)(S_3-T_3) + 14(F_3+H_3)\right]\right\} \tag{35}$$

and

$$U_{\eta\eta,L_3} = n - \left[(1-\mu)(1-3D_{L_3}\delta_{L_3})T_3 + S_3\mu(1-3E_3\delta_{L_3})\right]$$
$$-\frac{3}{2}\left[\mu G_3 A_2(1-5E_3\delta_{L_3}) + (1-\mu)(2\sigma_1-\sigma_2)(1-5D_3\delta_{L_3})Q_3\right] - 3(1-\mu)(\sigma_1-\sigma_2)(1-5D_3\delta_{L_3})Q_3$$
$$+\frac{1}{c^2}\left\{\frac{(1-b_3-\mu)^2}{2}\left[1-3\left(T_3(1-\mu)+S_3\mu\right)\right] - (\mu-\mu^2-3)\right.$$
$$+3\left[E_3\mu + D_3(1-\mu)\right] + \left[S_3\mu + T_3(1-\mu)\right]\left[E_3\mu + D_3(1-\mu)\right]$$
$$\left.+\frac{\mu(1-\mu)}{2}\left[T_1 + (-6+4\mu+7b_3)(S_3-T_3) + 2\left(S_3(1-\mu)+T_3\mu\right)\right]\right\} \tag{36}$$

where $D_3, E_3, F_3, G_3, H_3, J_3, Q_3, S_3, T_3$ and W_3 are all functions of μ

2.5 Solution of the Characteristic eq. (9)

Recalling eq. (9)

$$\lambda^4 - \mathrm{N}_{L_\alpha}\lambda^2 + \mathrm{M}_{L_\alpha} = 0, \quad \alpha = 1,2,3$$

where N_{L_α} and M_{L_α} are given by eq. (14*a*). Among several methods, we carry out the stability analysis based on the linearized equations by considering roots of the characteristic equation. For $L_\alpha, \alpha = 1,2,3$, we computed the numerical values of M_{L_α}, in the

interval $\mu \in (0.0.5)$. In all cases we obtained $\mathrm{M}_{L_\alpha} = U_{\xi\xi,L_\alpha}U_{\eta\eta,L_\alpha} < 0$ which leads to two real and two imaginary roots of the characteristic equation.

Therefore, under considered perturbations, the collinear points are unstable as in the classical RTBP. The following tables (1 – 2) show the obtained solutions. Each solution corresponds to one of the collinear points. For several values σ_1, σ_2 and A_2 we also sketched the variations in $U_{\xi\xi,L_\alpha}U_{\eta\eta,L_\alpha}$ versus the mass ratio μ in each case.

2.6 Numerical Representations and Analyses for Stability of $L_\alpha, \alpha = 1,2,3$

A program is constructed using *Mathematica* 9 software package so as to draw the variations in $U_{\xi\xi}U_{\eta\eta}$ of $L_\alpha, \alpha = 1,2,3$ versus the whole range of the mass ratio μ taking into account the oblateness effects A_2, the triaxial effect σ_1, σ_2 and the relativistic corrections.

Analysis of the Fig. 5 and Fig. 6

The curve in Fig.5 shows that the $U_{\xi\xi}U_{\eta\eta} < 0$ for whole domain of the mass ratio, i.e., L_1 is still unstable as is known in RTBP. Its magnitude is increasing with respect to the increase in the mass ratio. While in Fig. 6, the curve shows that the $U_{\xi\xi}U_{\eta\eta} < 0$ for whole domain of the mass ratio, i.e., L_2 is still unstable as is known in RTBP. Its magnitude is decreasing with respect to the increase in the mass ratio.

Analysis of the Fig. 7 and Fig. 8

In Fig. 7, the bigger the gravitational harmonics σ_1, σ_2, A_2 the bigger the perturbations on $U_{\xi\xi}U_{\eta\eta}$ but it still negative $U_{\xi\xi}U_{\eta\eta} < 0$ for whole domain of the mass ratio,

Table 1. The roots of the characteristic equations for points $L_\alpha, \alpha = 1,2,3$ for different values of σ_1, σ_2, $A_2 = 0.001$ and $\mu = 0.35$

Triaxiality Coefficients	λ's	Roots L_1	Roots L_2	Roots L_3
$\sigma_1 = 0.04$ $\sigma_2 = 0.04$	λ_3	-4.1710	-1.4950	-0.9917
	λ_4	4.1710	1.4950	0.9917
	λ_1	-3.0283i	-1.4489i	-0.9832i
	λ_2	3.0283i	1.4489i	0.9832i
$\sigma_1 = 0.04$ $\sigma_2 = 0.03$	λ_3	-4.2665	-1.5242	-1.1761
	λ_4	4.2665	1.5242	1.1761
	λ_1	-3.1153i	-1.4551i	-1.2237i
	λ_2	3.1153i	1.4551i	1.2237i
$\sigma_1 = 0.03$ $\sigma_2 = 0.025$	λ_3	-4.1252	-1.4809	-1.1070
	λ_4	4.1252	1.4809	1.1070
	λ_1	-3.0307i	-1.4471i	-1.2156i
	λ_2	3.0307i	1.4471i	1.2156i
$\sigma_1 = 0.02$ $\sigma_2 = 0.015$	λ_3	-4.0277	-1.4523	-1.0697
	λ_4	4.0277	1.4523	1.0697
	λ_1	-2.9898i	-1.4427i	-1.2286i
	λ_2	2.9898i	1.4427i	1.2286i
$\sigma_1 = 0.01$ $\sigma_2 = 0.0075$	λ_3	-3.8982	-1.4167	-1.0143
	λ_4	3.8982	1.4167	1.0143
	λ_1	-2.9258i	-1.4375i	-1.2332i
	λ_2	2.9258i	1.4375i	1.2332i

Table 2. The roots of the characteristic equations for points $L_\alpha, \alpha = 1,2,3$ for versus $\mu \in (0.04, 0.48)$, $A_2 = 0.001$, $\sigma_1 = 0.03$ and $\sigma_1 = 0.025$

μ	λ's	Roots L_1	Roots L_2	Roots L_3	μ	Roots L_1	Roots L_2	Roots L_3
0.04	λ_3	-3.5786	-2.1364	-0.4477	0.24	-4.0377	-1.6484	-0.9094
	λ_4	3.5786	2.1364	0.4477		4.0377	1.6484	0.9094
	λ_1	-2.6781i	-1.8009i	-0.9505i		-2.9809i	-1.5365i	-1.1274i
	λ_2	2.6781i	1.8009i	0.9505i		2.9809i	1.5365i	1.1274i
0.08	λ_3	-3.7330	-1.9879	-0.5743	0.32	-4.1075	-1.5240	-1.0487
	λ_4	3.7330	1.9879	0.5743		4.1075	1.5240	1.0487
	λ_1	-2.7852i	-1.7218i	-0.9929i		-3.0214i	-1.4699i	-1.1890i
	λ_2	2.7852i	1.7218i	0.9929i		3.0214i	1.4699i	1.1890i
0.12	λ_3	-3.8416	-1.8817	-0.6742	0.36	-4.1302	-14669	-1.1290
	λ_4	3.8416	1.8817	0.6742		4.1302	1.4669	1.1290
	λ_1	-2.8570i	-1.6638i	-1.0303i		-3.0331i	-1.4398i	-1.2257i
	λ_2	2.8570i	1.6638i	1.0303i		3.0331i	1.4398i	1.2257i
0.16	λ_3	-3.9236	-1.7943	-0.7601	0.4	-4.1461	-1.4122	-1.2476
	λ_4	3.9236	1.7943	0.7601		4.1461	1.4122	1.2476
	λ_1	-2.9098i	-1.6159i	-1.0646i		-3.0401i	-1.4112i	-1.2816i
	λ_2	2.9098i	1.6159i	1.0646i		3.0401i	1.4112i	1.2816i
0.2	λ_3	-3.9874	-1.7177	-0.8375	0.48	-4.1609	-1.3088	-2.2503

λ_4	3.9874	1.7177	0.8375	4.1609	1.3088	2.2503
λ_1	-2.9501i	-1.5741i	-1.0967i	-3.0417i	-1.3580i	-1.8062i
λ_2	2.9501i	1.5741i	1.0967i	3.0417i	1.3580i	1.8062i

i.e., L_1 is still unstable as is known in RTBP. The magnitude of $U_{\xi\xi}U_{\eta\eta}$ is decreasing for a very short interval of mass ratio, then increasing with respect to the increase in the mass ratio. While in Fig. 8, the curve shows that the $U_{\xi\xi}U_{\eta\eta} < 0$ for whole domain of the mass ratio, i.e., L_2 is still unstable as is known in RTBP. Its magnitude is decreasing with respect to the increase in the mass ratio.

Analysis of the Fig. 9 and Fig. 10

In Fig. 9, Considering the oblateness effect only and ignoring the triaxiality effects we get the smallest effects in magnitude on $U_{\xi\xi}U_{\eta\eta}$, while ignoring the oblateness and considering only the triaxiality perturbations we get the largest effects in magnitude on $U_{\xi\xi}U_{\eta\eta}$, but it still negatives i.e.

$U_{\xi\xi}U_{\eta\eta} < 0$ for whole domain of the mass ratio, i.e., L_1 is still unstable as is known in RTBP. The general trend of all curves are as follows: the bigger the gravitational harmonics σ_1, σ_2, A_2 the bigger the perturbations on $U_{\xi\xi}U_{\eta\eta}$ The magnitude of $U_{\xi\xi}U_{\eta\eta}$ is decreasing for a very short interval of mass ratio, then increasing with respect to the increase in the mass ratio. While in Fig. 10, the dynamics of $U_{\xi\xi}U_{\eta\eta}$ seems inverse of Fig. 7, but the dynamical behavior of L_2 does not change from.

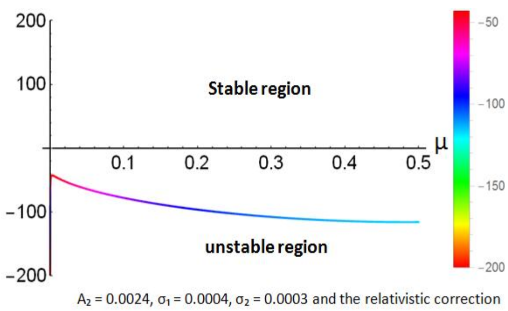

Fig. 5. The variations in $U_{\xi\xi}U_{\eta\eta}$ of L_1 point versus the mass ratio μ at $A_2 = 0.0024$, $\sigma_1 = 0.0004$, $\sigma_2 = 0.0003$ and relativistic corrections

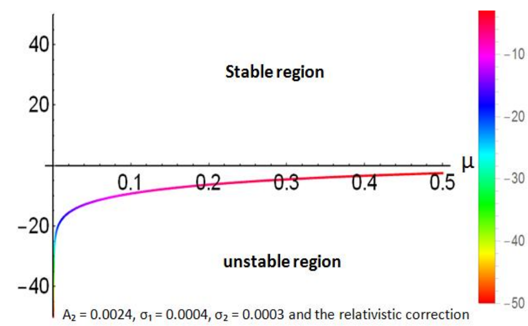

Fig. 6. The variations in $U_{\xi\xi}U_{\eta\eta}$ of L_2 point versus the mass ratio μ at $A_2 = 0.0024$, $\sigma_1 = 0.0004$, $\sigma_2 = 0.0003$ and relativistic corrections

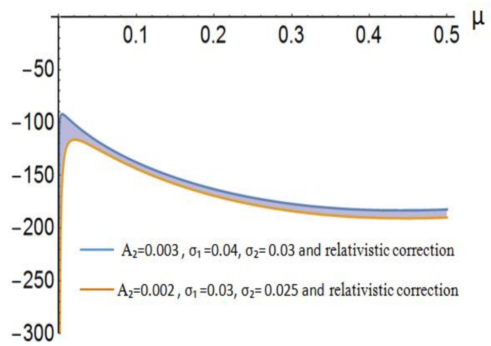

Fig. 7. The variations in $U_{\xi\xi}U_{\eta\eta}$ of L_1 point versus the mass ratio μ , at different values σ_1, σ_2, A_2 and relativistic corrections

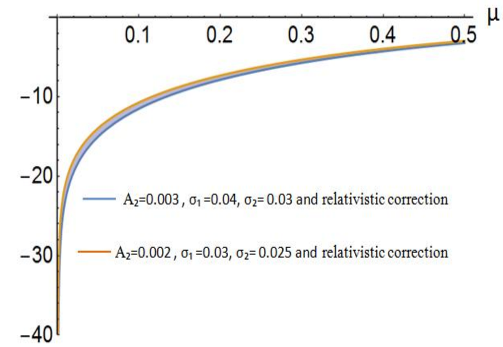

Fig. 8. The variations in $U_{\xi\xi}U_{\eta\eta}$ of L_2 point versus the mass ratio μ , at different values σ_1, σ_2, A_2 and relativistic corrections

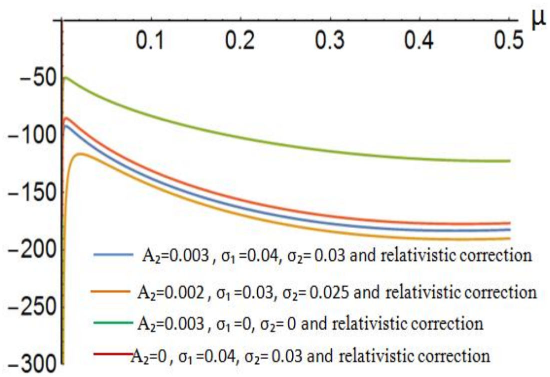

Fig. 9. The variations $U_{\xi\xi}U_{\eta\eta}$ of L_1 point versus the mass ratio μ at different values σ_1, σ_2, A_2 and relativistic corrections

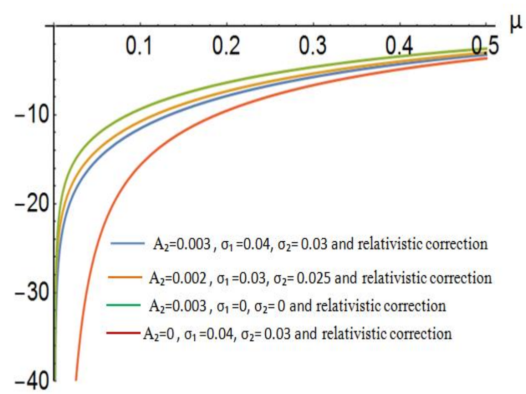

Fig. 10. The variations in $U_{\xi\xi}U_{\eta\eta}$ of L_2 point versus the mass ratio μ at different values σ_1, σ_2, A_2 and relativistic corrections

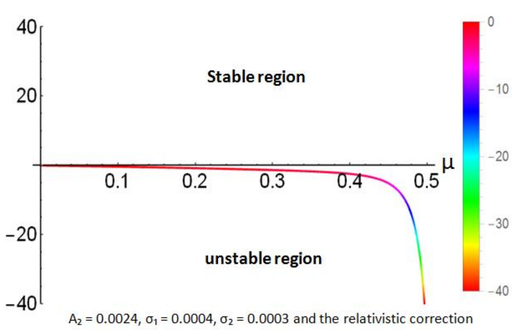

Fig. 11. The variations in $U_{\xi\xi}U_{\eta\eta}$ of L_3 point versus the mass ratio μ at $A_2 = 0.0024$, $\sigma_1 = 0.0004$, $\sigma_2 = 0.0003$ and relativistic corrections

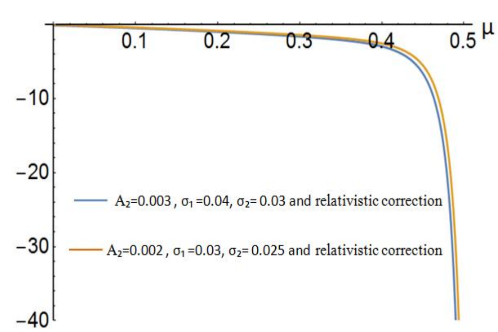

Fig. 12. The variations in $U_{\xi\xi}U_{\eta\eta}$ of L_3 point versus the mass ratio μ at different values σ_1, σ_2, A_2 and relativistic corrections

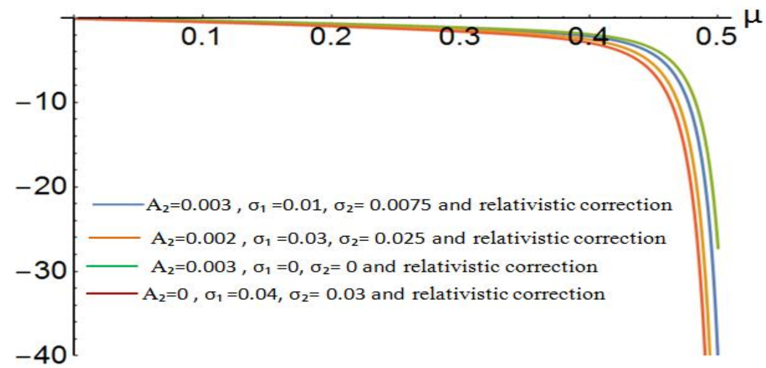

Fig. 13 The variations in $U_{\xi\xi}U_{\eta\eta}$ of L_3 point versus the mass ratio μ at different values σ_1, σ_2, A_2 and relativistic corrections

Analysis of the Fig. 11, Fig. 12 and Fig. 13

The curve in Fig. 11 shows that the $U_{\xi\xi}U_{\eta\eta} < 0$ for whole domain of the mass ratio, i.e., L_3 is still unstable as is known in RTBP. Its magnitude is increasing with respect to the increase in the mass ratio. While in Fig.12, the curve shows that the $U_{\xi\xi}U_{\eta\eta} < 0$ for whole domain of the mass ratio, i.e., L_3 is still unstable as is known in RTBP. Its magnitude is increasing with respect to the increase in the mass ratio. The effect of changing the oblateness and the triaxiality of the primaries are clear from the figures, see Fig.12. In Fig.13 Considering the oblateness effect only and ignoring the triaxiality effects we get the smallest effects in magnitude on $U_{\xi\xi}U_{\eta\eta}$, while ignoring the oblateness and considering only the triaxiality perturbations we get the largest effects in magnitude on $U_{\xi\xi}U_{\eta\eta}$, but it still negative i.e. $U_{\xi\xi}U_{\eta\eta} < 0$ for whole domain of the mass ratio, i.e. L_3 is still unstable as is known in RTBP.

3. CONCLUSION

In conclusion, firstly, we have treated the problem of the stability of collinear equilibrium points of the RTBP under the influence of triaxiality of the more massive primary, oblateness of the less massive primary and the relativistic corrections. Secondly, we have built up the potential like function of the problem and computed the mean motion of the problem. Moreover, we have constructed the equations of motion of the problem. To study the stability of the current problem, we linearized the equations of motion around the collinear points. In addition, we have derived the characteristic equation of the collinear points. Our study revealed the existence of two real and two imaginary roots of the characteristic equation as deduced from the plotted figures in the manuscript. We have computed some selected roots corresponding to the eigenvalues based on some selected values of the perturbing parameters. These eigenvalues have reflected the instability nature of the collinear points. Finally, as seen from the curves plotted in Figs. 5- 13, that the value of $\mathrm{M}_{L_\alpha} = U_{\xi\xi,L_\alpha} U_{\eta\eta,L_\alpha}$ is negative in the whole domain of the mass ratio $\mu \in (0, 0.5)$ under the considered model of perturbations. i.e., it ensures the negativity of $U_{\xi\xi}U_{\eta\eta}$ thus the conclusion of instability of the collinear points is true. Also, tables 1 and 2 revealed the existence of two real and two imaginary roots of the characteristic equation that means the collinear points are unstable.

COMPETING INTERESTS

Author has declared that no competing interests exist.

REFERENCES

1. Szebehely VG. Theory of orbits. Yale University, New Haven, Connecticut, Academic Press, New-York and London, The Restricted Problem of Three Bodies;1967.
2. Euler L. On the rectilinear motion of three bodies mutually attracted to each other; 1767.
3. Lagrange J. L.Essai sur le Problème des Trois Corps, Oeuvres de Lagrange, Acad. Roy. 1772;6:229-332.
4. Brumberg V. Relativistic celestial mechanics, rcm; 1972.

5. Brumberg V. Essential relativistic celestial mechanics. CRC Press; 1991.
6. Maindl TI, Dvorak R. On the dynamics of the relativistic restricted three-body problem, Astronomy and Astrophysics, 1994;290:335–339.
7. Ragos O, Perdios EA, Kalantonis VS, Vrahatis MN. On the equilibrium points of the relativistic restricted three-body problem, Nonlinear Analysis: Theory, Methods & Applications, 2001;47:3413–3418.
8. Douskos CN, Perdios EA. On the stability of equilibrium points in the relativistic restricted three-body problem. Celestial Mechanics and Dynamical Astronomy. 2002;82:317–321.
9. Ahmed MK, Abd El-Salam FA, Abd El-Bar SE. On the stability of the triangular Lagrangian equilibrium points in the relativistic restricted three-body problem. American Journal of Applied Sciences. 2006;3:1993–1998.
10. Ishwar B, Kushvah BS. Linear Stability of Triangular Equilibrium Points in the Generalized Photo gravitational restricted three body problem with poynting roberts on drag. Journal of Dynamical Systems and Geometric Theories. 2006;4:79–86.
11. Namboodiri NIV, Reddy DS, Sharma RK. Effect of oblateness and radiation pressure on angular frequencies at collinear points, Astrophysics and Space Science. 2008;318:161–168.
12. Mittal A, Ahmad I, Bhatnagar KB. Periodic orbits in the photo gravitational restricted problem with the smaller primary an oblate body. Astrophysics and Space Science. 2009;323:65–73.
13. Kumar S, Ishwar B. Solutions of generalized photo gravitational elliptic restricted three body problem, in AIP Conference Proceedings. 2009;1146:456–461.
14. Abd El-Bar SE, Abd El-Salam FA. Combined effects of oblateness and photogravitational perturbations on the stability of the equilibrium points in the relativistic RTBP,Candian Joural of Physics. 2019;97:231–240.
15. Abd El-Bar SE, Abd El-Salam FA, Al-Burkani AM. Computation of the perturbed locations of L1 for all Sun-Planet RTBP systems with oblate primaries, Results in Physics. 2019;102659. DOI: 10.1016/j.rinp.2019.102659.
16. Elshaboury SM, Abouelmagd EI, Kalantonis VS, Perdios EA. The planar restricted three-body problem when both primaries are triaxial rigid bodies: Equilibrium points and periodic orbits. Astrophysics and Space Science. 2016;361.
DOI: 10.1007/s10509-016-2894-x
17. Martínez R, Simó C. Relative equilibria of the restricted three-body problem in curved spaces. Celestial Mechanics and Dynamical Astronomy. 2017;128:221–259.
18. Bhatnagar KB, Hallan PP. Existence and stability of L 4, 5 in the relativistic restricted three-body problem. Celestial Mechanics and Dynamical Astronomy. 1997;69:271–281.

Appendix A

$$\mathrm{F}_{-3}^{(1)}=\frac{81A_2^2}{4},\qquad \mathrm{F}_{-2}^{(1)}=-\frac{9A_2}{2}-\frac{27BA_2}{4}+\frac{9n^2A_2}{2}-\frac{567A_2^2}{4}$$

$$\mathrm{F}_{-1}^{(1)}=\frac{93A_2}{2}+36BA_2-\frac{327n^2A_2}{8}+\frac{1971A_2^2}{4}$$

$$\mathrm{F}_{0}^{(1)}=-3B-\frac{9B^2}{4}+\frac{3n^2}{4}+\frac{9Bn^2}{8}+\frac{n^4}{4}-\frac{877A_2}{4}-87BA_2+\frac{727n^2A_2}{4}-\frac{5139A_2^2}{4}$$

$$\mathrm{F}_{1}^{(1)}=\frac{15}{2}+\frac{57B}{4}+\frac{9B^2}{4}-\frac{23n^2}{4}-\frac{27Bn^2}{4}-\frac{11n^4}{4}+\frac{4057A_2}{6}+\frac{715BA_2}{4}-\frac{13345n^2A_2}{24}+2889A_2^2$$

$$\mathrm{F}_{2}^{(1)}=-\frac{67}{2}-\frac{65B}{2}-\frac{3B^2}{4}+\frac{115n^2}{6}+\frac{153Bn^2}{8}+\frac{44n^4}{3}-\frac{59303A_2}{36}-\frac{4399BA_2}{12}+\frac{12059n^2A_2}{9}-\frac{22125A_2^2}{4}$$

$$F_3^{(1)} = \frac{802}{9} + \frac{847B}{12} + \frac{53B^2}{4} - \frac{1481n^2}{36} - \frac{327Bn^2}{8} - \frac{1831n^4}{36} + \frac{362623A_2}{108} + \frac{5306BA_2}{9} + 9042A_2^2 - \frac{285187n^2A_2}{108}$$

$$F_4^{(1)} = -200 - 126B - \frac{45B^2}{4} + \frac{413n^2}{6} + \frac{147Bn^2}{2} + \frac{4571n^4}{36} - \frac{925739A_2}{162} - \frac{21113BA_2}{27} + \frac{1381897n^2A_2}{324} - \frac{154879A_2^2}{12}$$

$$F_5^{(1)} = \frac{18911}{54} + 167B + 3B^2 - \frac{2426n^2}{27} - \frac{797Bn^2}{8} - \frac{24991n^4}{108} + \frac{1983367A_2}{243} + \frac{312743BA_2}{324} - \frac{2713313n^2A_2}{486} + \frac{143101A_2^2}{9}$$

$$F_6^{(1)} = -\frac{238415}{486} - \frac{64535B}{324} - \frac{39B^2}{2} + \frac{22822n^2}{243} + \frac{589Bn^2}{6} + \frac{22696n^4}{81} - \frac{28183715A_2}{2916} - \frac{239344BA_2}{243} + \frac{4117370n^2A_2}{729} - \frac{15905525A_2^2}{972}$$

$$F_7^{(1)} = \frac{28553}{54} + \frac{14774B}{81} + \frac{45B^2}{4} - \frac{27197n^2}{243} - \frac{257Bn^2}{4} - \frac{1273n^4}{12} + \frac{39055031A_2}{4374} + \frac{554072BA_2}{729} - \frac{65765321n^2A_2}{17496} + \frac{12948929A_2^2}{972}$$

$$F_8^{(1)} = -\frac{274523}{729} - \frac{5429B}{54} - \frac{3B^2}{2} + \frac{596533n^2}{2916} + \frac{461Bn^2}{72} - \frac{11426n^4}{27} - \frac{141223105A_2}{26244} - \frac{1750135BA_2}{4374} + \frac{2563681n^2A_2}{6561} - \frac{5209148A_2^2}{729}$$

$$F_9^{(1)} = \frac{69206}{2187} - \frac{1885B}{2916} - \frac{288356n^2}{729} + \frac{5333Bn^2}{162} + \frac{1084129n^4}{972} + \frac{2174641A_2}{39366} + \frac{71BA_2}{13122} + \frac{93188009n^2A_2}{39366} + \frac{863A_2^2}{2916}$$

Appendix B

$$G_{-3}^{(2)} = -\frac{81A_2^2}{4}, \qquad G_{-2}^{(2)} = -\frac{9A_2}{2} - \frac{27BA_2}{4} - \frac{9n^2A_2}{2} - \frac{567A_2^2}{4}$$

$$G_{-1}^{(2)} = -\frac{93A_2}{2} - 36BA_2 - \frac{345n^2A_2}{8} - \frac{1971A_2^2}{4}$$

$$G_0^{(2)} = -3B - \frac{9B^2}{4} - \frac{5n^2}{4} - \frac{15Bn^2}{8} - \frac{n^4}{4} - \frac{479A_2}{2} - 87BA_2 - \frac{805n^2A_2}{4} - \frac{3681A_2^2}{4}$$

$$G_1^{(2)} = -12 - 21B - \frac{9B^2}{4} - \frac{63n^2}{4} - \frac{45Bn^2}{4} - \frac{11n^4}{4} - \frac{2177A_2}{3} - \frac{283BA_2}{4} - \frac{13591n^2A_2}{24} - 621A_2^2$$

$$G_2^{(2)} = -71 - 55B - \frac{3B^2}{4} - 86n^2 - \frac{255Bn^2}{8} - \frac{44n^4}{3} - \frac{48017A_2}{36} + \frac{1649BA_2}{12} - \frac{9005n^2A_2}{9} + \frac{5469A_2^2}{4}$$

$$G_3^{(2)} = -\frac{4133}{18} - \frac{757B}{12} + \frac{55B^2}{4} - \frac{9931n^2}{36} - \frac{359Bn^2}{8} - \frac{1777n^4}{36} - \frac{65279A_2}{54} + \frac{4090BA_2}{9} - \frac{107995n^2A_2}{108} + 4188A_2^2$$

$$G_4^{(2)} = -\frac{2711}{6} + 22B + \frac{45B^2}{4} - \frac{5156n^2}{9} - \frac{35Bn^2}{2} - \frac{4229n^4}{36} + \frac{166043A_2}{324} + \frac{25139BA_2}{54} - \frac{78325n^2A_2}{324} + \frac{55721A_2^2}{12}$$

$$G_5^{(2)} = -\frac{15115}{27} + \frac{1951B}{12} + 3B^2 - \frac{21887n^2}{27} + \frac{905Bn^2}{24} - \frac{23497n^4}{108} + \frac{724733A_2}{243} - \frac{15743BA_2}{324} + \frac{244105n^2A_2}{486} + \frac{6803A_2^2}{9}$$

$$G_6^{(2)} = -\frac{177809}{486} + \frac{62437B}{324} - 21B^2 - \frac{429545n^2}{486} + \frac{697Bn^2}{18} - \frac{28960n^4}{81} + \frac{10534933A_2}{2916} - \frac{140848BA_2}{243} - \frac{116210n^2A_2}{729} - \frac{3877025A_2^2}{972}$$

$$G_7^{(2)} = -\frac{8141}{162} + \frac{19063B}{324} - \frac{45B^2}{4} - \frac{178025n^2}{162} - \frac{425Bn^2}{12} - \frac{21469n^4}{36} + \frac{3256961A_2}{2187} - \frac{355163BA_2}{729} - \frac{36834215n^2A_2}{17496} - \frac{4233653A_2^2}{972}$$

$$G_8^{(2)} = -\frac{100105}{1458} - \frac{16265B}{324} - \frac{3B^2}{2} - \frac{5596727n^2}{2916} - \frac{17113Bn^2}{216} - \frac{27773n^4}{27} - \frac{14087719A_2}{26244} - \frac{127451BA_2}{2187} - \frac{22945408n^2A_2}{6561} - \frac{874352A_2^2}{729}$$

$$G_9^{(2)} = \frac{969374}{2187} + \frac{2665B}{2916} - \frac{7145969n^2}{2187} - \frac{26345Bn^2}{486} - \frac{1680113n^4}{972} - \frac{1678094A_2}{19683} - \frac{71BA_2}{13122} - \frac{157236505n^2A_2}{39366} - \frac{863A_2^2}{2916}$$

Appendix C

$$J_3^{(3)} = -\frac{69}{16} - \frac{651B}{32} - \frac{279B^2}{16} - \frac{79n^2}{16} - \frac{561Bn^2}{32} - \frac{15n^4}{8} + \frac{9A_2}{64} + \frac{81BA_2}{128} + \frac{27n^2A_2}{128}$$

$$J_6^{(3)} = \frac{3661}{128} + \frac{23949B}{256} + \frac{351B^2}{8} + \frac{4291n^2}{128} + \frac{261Bn^2}{4} + \frac{315n^4}{64} - \frac{81A_2}{32} - \frac{5535BA_2}{1024} - \frac{261n^2A_2}{128} + \frac{81A_2^2}{2048}$$

$$J_9^{(3)} = \frac{13419}{128} + \frac{199339B}{1024} + \frac{39669B^2}{1024} + \frac{172543n^2}{1536} + \frac{256655Bn^2}{2048} + \frac{3087n^4}{512} - \frac{3591A_2}{256} - \frac{132489BA_2}{8192} - \frac{17325n^2A_2}{2048} + \frac{6237A_2^2}{16384}$$

Peer-review history:
The peer review history for this paper can be accessed here:
http://www.sdiarticle4.com/review-history/66192